
TOKENIZING LOOPS OF ANTIBODIES

Ada Fang^{1,2†} Robert G. Alberstein² Simon Kelow² Frédéric A. Dreyer²

¹Harvard University ²Prescient Design, Genentech

[†]Work done during an internship at Prescient Design, Genentech.

ABSTRACT

The complementarity-determining regions (CDRs) of antibodies are loop structures that are key to their interactions with antigens, and of high importance to the design of novel biologics. Since the 1980s, categorizing the diversity of CDR structures into canonical clusters has enabled the identification of key structural motifs of antibodies. However, existing approaches have limited coverage and cannot be readily incorporated into protein foundation models. Here we introduce **ImmunoGlobulin LOOp** Tokenizer, **IGLOO**, a multimodal antibody loop tokenizer that encodes backbone dihedral angles and sequence. IGLOO is trained using a contrastive learning objective to map loops with similar backbone dihedral angles closer together in latent space. Compared to state-of-the-art protein encoding approaches, IGLOO can efficiently retrieve the closest matching loop structures from a structural antibody database, outperforming the existing methods on identifying similar H3 loops by 5.9%. IGLOO assigns tokens to all loops, addressing the limited coverage issue of canonical clusters, while retaining the ability to recover canonical loop conformations. To demonstrate the versatility of IGLOO tokens, we show that they can be incorporated into protein language models with IGLOOLM and IGLOOALM. On predicting binding affinity of heavy chain variants, IGLOOLM outperforms the base protein language model on 8 out of 10 antibody-antigen targets. Additionally, it is on par with existing state-of-the-art sequence-based and multimodal protein language models, performing comparably to models with $7\times$ more parameters. IGLOOALM samples antibody loops which are diverse in sequence and more consistent in structure than state-of-the-art antibody inverse folding models. IGLOO demonstrates the benefit of introducing multimodal tokens for antibody loops for encoding the diverse landscape of antibody loops, improving protein foundation models, and for antibody CDR design.

1 INTRODUCTION

Antibodies are a class of proteins that are essential in the body’s immune response and a widely used therapeutic modality (Crescioli et al., 2025). They are comprised of two identical light and two identical heavy chains. The light and heavy chains are divided into a constant and variable domain, where the variable domain is comprised of complementarity-determining regions (CDRs),¹ which are structurally distinct flexible loops between antiparallel beta strands in the immunoglobulin fold. The CDRs play an essential role in the antibody’s ability to recognize and bind antigens in a highly specific manner (Xu & Davis, 2000). Protein and antibody language models trained on amino acid sequence tokens have been powerful for learning evolutionary patterns that are useful for function prediction (Kulmanov et al., 2024), sequence design (Zhao et al., 2025b), and variant effect prediction (Hie et al., 2024; Notin et al., 2023).

Recently, the development of multimodal protein language models (Su et al., 2023; Heinzinger et al., 2024; Hayes et al., 2025) has expanded to incorporate structure tokens in addition to sequence tokens. However, such approaches tokenize structures at the amino acid level, focus on reconstruction, and do not consider the higher-level organization and modularity of protein domains (Sigrist et al., 2010; Mistry et al., 2021). A multimodal tokenizer for antibodies should therefore consider the inherent organisation in antibody structures and sequences for effective representation learning.

¹Here we consider four CDR regions. The fourth CDR is the loop joining the D and E strands adjacent to CDR1 and CDR2, which is often considered part of the framework (Kelow et al., 2020).

Tokenization or clustering of immunoglobulin loop regions based on their dihedral backbone angles into ‘canonical clusters’ has been adopted since Chothia & Lesk (1987). Such a grouping of loops has been useful for understanding the structural diversity of antibodies (Teplyakov et al., 2016), designing antibody loops with consistent structure and diverse sequences (Adolf-Bryfogle et al., 2018), and for studying conformational changes of antibody loops in MD simulations (Fernández-Quintero et al., 2020; 2019). These approaches are limited by their (1) limited coverage of antibody structures, with 20.3% of all loops having no known matching canonical cluster, including 76.3% of H3 loops (Table S5), (2) all existing clusters only consider backbone coordinates or dihedral angles, without incorporating sequence information, and (3) existing clusters cannot be readily applied to protein language models. Thus, the tokenization of immunoglobulin loops for multimodal representation remains an open challenge.

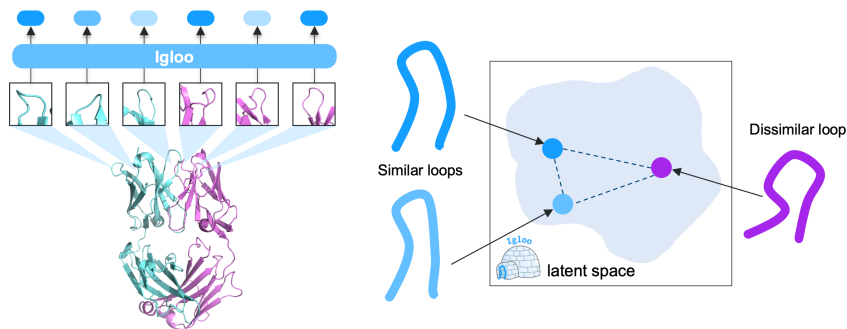


Figure 1: **Left** IGLOO is a multimodal tokenizer for antibody loops. **Right** Organization of the IGLOO latent space is achieved through a contrastive learning objective on dihedral angle distance between backbones.

Present work. We introduce **ImmunoG**lobulin **LOOp** Tokenizer, **IGLOO**, a *multimodal antibody loop tokenizer* for encoding backbone dihedral angles and sequence (Fig. 1). Unlike existing structure tokenizers, which focus on the amino acid scale, IGLOO tokenizes at the substructure loop level. IGLOO is trained on 807,815 loop regions from heavy and light chains of experimentally-derived and computationally predicted structures. We develop a contrastive learning objective based on the dihedral angle distance defined by North et al. (2011) to train IGLOO. While being a self-supervised model, IGLOO successfully reproduces known canonical conformations assigned for 90.6% of loops in SABDab Dunbar et al. (2014). To demonstrate the versatility and utility of IGLOO tokens, we present three key applications:

- **Retrieval of similar loop structures from large structural databases.** By learning to compare loop structures, IGLOO retrieves more similar loop structures from SABDab compared to state-of-the-art protein encoding approaches. For the H3 loop, which exhibits the most sequence and structure diversity, IGLOO outperforms the previous best model on retrieving H3 loops with similar dihedral angle backbones by 5.9%.
- **Improved antibody affinity prediction with protein language models.** We incorporate IGLOO loop tokens into an antibody language model, and train IGLOOLM. By using the representations learned from IGLOOLM to predict binding affinity of heavy chain variants, we show it outperforms the base model on 8 out of 10 antibody-antigen targets and performs on par to models with $7\times$ more parameters.
- **Sampling diverse loops with consistent structure.** IGLOOALM is a protein language model with the IGLOO loop tokens and IGLOO multimodal residue tokens. When loop sequences are masked out, the loops sampled from IGLOOALM are diverse in sequence and more consistent in structure than state-of-the-art antibody inverse folding models. Re-designed CDR H3 loops of a SARS-CoV-2 antibody with IGLOOALM achieves an average sequence identity of 0.27 while achieving less than 1Å RMSD to the original loop.

By introducing multimodal tokens for antibody loops, IGLOO captures the structural and functional diversity of loop conformations, improving the expressiveness of protein foundation models and advancing rational antibody design.

2 RELATED WORK

Tokenization of protein structure. The construction of classifications of protein structures at the domain level has been applied for understanding the relationship with domain function (Lo Conte et al., 2000; Ouzounis et al., 2003; Sigrist et al., 2010; Mistry et al., 2021). Learning structurally informed residue-level representations can be achieved with geometric features (Jing et al., 2020), multiview contrastive learning between sequence and structure views of the same protein (Zhang et al., 2022), hierarchical graph neural network on the protein structure (Wang et al., 2022), and with intermolecular interactions (Fang et al., 2025). Tokenization at the amino acid level has shown significant advances in the speed of protein structure search with Foldseek (Van Kempen et al., 2024). Yuan et al. (2025) compare different approaches for tokenizing amino acid structures including VQVAE (Hayes et al., 2025) and inverse-folding-based methods (Dauparas et al., 2022).

Multimodal protein language models. Multimodal protein language models have been trained to learn meaningful representations and to generate over sequence, structure, and function. Models such as SaProt (Su et al., 2023) and ProST5 (Heinzinger et al., 2024) learn representations from protein sequence and Foldseek 3Di amino acid tokens, which capture structural information. ProSST (Li et al., 2024) represents proteins with sequence and residue-level structure tokens that capture local environments. ProSSN (Tan et al., 2025) uses both sequence and the topological structure of proteins to learn multimodal representations. ESM3 (Hayes et al., 2025) is a generative model that models the sequence, structure, and function of amino acids simultaneously.

Clustering Immunoglobulin Loops. The CDRs of antibodies demonstrate the most variability and are essential to the binding of antibodies to antigens. Thus, there has been significant effort in categorizing all known structures of CDRs (Chothia & Lesk, 1987; Shirai et al., 1996; North et al., 2011; Adolf-Bryfogle et al., 2015; Nowak et al., 2016; Wong et al., 2019b; Kelow et al., 2022; Liu et al., 2024). CDRs fold into a loop structure, and a pair of loops can be compared through their backbone dihedral angles (North et al., 2011). While most approaches only cluster loops of the same length, Nowak et al. (2016) explore clustering of loops of different lengths by aligning loops with their stem region (subsequence of amino acids before and after the loop region) and comparing the resultant RMSD between the loops. SCALOP (Wong et al., 2019a) predicts canonical loops from protein sequences for large-scale annotation of antibody libraries. Zhang et al. (2025) train their model to learn the RMSD between pairs of loops and show how it can be used for designing CDRs. Current methods are limited as many CDRs, especially H3 loops, do not have known canonical conformations (Table S5). We extend existing approaches through the self-supervised definition of antibody loop clusters.

3 METHOD

IGLOO is a multimodal tokenizer that incorporates both sequence and backbone structure of the loop structures. Here we focus on modeling loops within antibodies and TCRs, which are the four CDRs of the heavy and light chains. IGLOO is a *tokenizing function* that maps for a loop sequence and backbone structure, to a token \mathbf{t} .

Problem definition. An antibody loop with n residues is defined by: (1) a sequence of amino acids $\mathbf{a} = (a_1, \dots, a_n)$ where $\forall i, a_i \in \mathcal{V} = \{\text{Ala}, \text{Arg}, \dots, \text{Tyr}, \text{Val}\}$, which are canonical amino acid residues, and (2) their backbone dihedral angles $\phi, \psi, \omega \in (-\pi, \pi]^n$ (Fig. 2). Our goal is to train a tokenizer $f(\cdot)$ for antibody loops such that $f(\mathbf{a}, \phi, \psi, \omega) = \mathbf{t}$, where $\mathbf{t} \in \mathbb{R}^d$ and d are the dimensions of the token embeddings. For the token \mathbf{t} , it can be used to determine loops that share a similar structure, incorporation into a protein language model, and for guided generation.

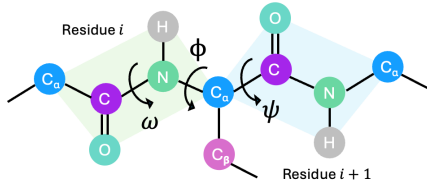


Figure 2: Backbone dihedral angles for residue i .

3.1 MULTIMODAL TOKENIZATION OF LOOPS

The input to IGLOO is a loop of length n with dihedral angles $(\phi, \omega, \psi) \in (-\pi, \pi]^{n \times 3}$ and amino acid identities \mathbf{a} . The dihedral angles are first converted into coordinates on the unit circle $(\cos \phi, \sin \phi, \cos \psi, \sin \psi, \cos \omega, \sin \omega) \in [-1, 1]^{n \times 6}$ and then projected with a linear layer $\mathbf{D} = (\cos \phi, \sin \phi, \cos \psi, \sin \psi, \cos \omega, \sin \omega) \mathbf{W}^{\text{dihedral}} + \mathbf{b}^{\text{dihedral}}$, where $\mathbf{D} \in \mathbb{R}^{n \times d}$, $\mathbf{W}^{\text{dihedral}} \in \mathbb{R}^{d \times 6}$, and $\mathbf{b}^{\text{dihedral}} \in \mathbb{R}^d$. For the loop sequence, it is encoded with 20 learnable embeddings for each of the canonical amino acid types into $\mathbf{A} \in \mathbb{R}^{n \times d}$. Next, we sum the sequence and dihedral angle embeddings to produce a multimodal embedding, $\mathbf{X} = \mathbf{D} + \mathbf{A} \in \mathbb{R}^{n \times d}$ (Fig. 3a). To learn a representation across the loop residues $\mathbf{X} = (\mathbf{x}_1, \dots, \mathbf{x}_n)$, we use a transformer architecture based on BERT (Devlin et al., 2019) using the ESM-2 implementation (Lin et al., 2023). A learnable classification token, \mathbf{t} , is added to the start of each sequence to learn a meaningful overall representation of the loop.

3.2 IGLOO SELF-SUPERVISED TRAINING OBJECTIVES

We train IGLOO with four objective functions (Fig. 3b): (1) masked reconstruction of dihedral angles, (2) masked reconstruction of amino acid identities, (3) contrastive learning of protein backbones, and (4) codebook learning. Following the multimodal masking approach of ESM-3 (Hayes et al., 2025), we randomly mask 30% of the input tokens and vary the masking patterns across tracks as described below, ensuring that IGLOO is exposed to every possible combination of tracks during reconstruction.

Masked reconstruction of dihedral angles. For masking of sequence tokens, the following approaches are used (1) Masking uniformly at random the dihedral angles and protein sequence for 20% of inputs, (2) masking uniformly at random only the dihedral angles for 20% of inputs, (3) completely masking the dihedral angles, keeping only the protein sequence for 10% of inputs. For dihedral angle θ_i of residue i in a loop, the predicted unit circle coordinates (x_i, y_i) are given by passing the hidden representation of the residue to a two-layer MLP. The reconstruction loss $\ell_{\text{dihedral recon. } i}$ is given by the mean squared error between $(\cos \theta_i, \sin \theta_i)$ and $(\cos \hat{\theta}_i, \sin \hat{\theta}_i)$, where $\hat{\theta}_i = \arctan(y_i/x_i)$. We also add a penalty term, $\ell_{\text{dihedral reg.}}$, to regularize the model for the reconstruction of coordinates on the unit circle (Pavilo et al., 2018).

Masked reconstruction of amino acid identities. We employ several variations of masking tokens across the inputs for 20% of inputs. (1) Masking uniformly at random the protein sequence and the dihedral angles, (2) masking uniformly at random only the protein sequence for 20% of inputs, (3) completely masking the protein sequence, keeping only the dihedral angles for 10% of inputs. The logits of the masked amino acids are given by passing the hidden representation of the residue to a two-layer MLP. The amino acid masking loss for amino acid i in a loop, $\ell_{\text{AA}, i}$, is given by the cross-entropy loss of the predicted amino acid identity and the true amino acid identity.

Contrastive learning of protein backbones. For IGLOO to learn a token, \mathbf{t} , such that similar tokens share similar loop conformations, we define a contrastive loss function. North et al. (2011) defines the similarity between two loops u and v of length n_u and n_v , respectively, and $n_u \leq n_v$. The loops have dihedral angles $(\phi^u, \psi^u, \omega^u) \in (-\pi, \pi]^{n_u \times 3}$ and $(\phi^v, \psi^v, \omega^v) \in (-\pi, \pi]^{n_v \times 3}$. The dihedral distance \mathcal{D} is defined as

$$\mathcal{D} = \frac{1}{3M} \sum_{\theta \in \{\phi, \psi, \omega\}} \sum_{i=1}^{n_u} 2(1 - \cos(\theta_i^u - \mathcal{P}(\theta_i^v))), \quad (1)$$

where \mathcal{P} aligns residues of loop v to residues of loop u . When $n_u = n_v$, the alignment is a one-to-one mapping between the residues. Otherwise, we define an alignment between the two loops using a dynamic time warping path (see Appendix D).

Proteins are chiral molecules, and the orientation of the backbone frame has a strong influence on the atomic structure through side-chain positioning. Prominent examples exist where the backbone RMSD of a pair of loops is low, yet dihedral angles can be up to 180° apart with opposite-pointing side chains (North et al., 2011). Therefore, we use dihedral angle distance \mathcal{D} over RMSD to capture the nuances of the loop structure.

A pair of loops u, v is a positive pair ($Y_{uv} = 1$) if the loops are of the same length and $\mathcal{D} < 0.1$. A pair of loops is a negative pair ($Y_{uv} = 0$) if they are of different lengths or $\mathcal{D} > 0.47$ for loops of the same length, where $\mathcal{D} = 0.47$ corresponds to an average difference in dihedral angles of 40° , which is the threshold used in the clustering by Kelow et al. (2022). Otherwise, the pair of loops is ignored. The *dihedral loss* is the mean binary cross-entropy over the pairs of loops in the batch with positive and negative labels.

$$\ell_{\text{contrastive}, uv} = \text{BCE}\left(\sigma\left(\frac{\mathbf{h}_u^\top \mathbf{h}_v}{\tau}\right), Y_{uv}\right), \quad (2)$$

where $\mathbf{h}_u = \frac{\mathbf{t}_u}{\|\mathbf{t}_u\|_2}$, \mathbf{t}_u is the classification token embedding for loop u in the batch, and τ is the temperature. We apply contrastive learning instead of predicting \mathcal{D} as the pretraining task for similar loops to be close in the latent space. A margin between positive and negative pairs is applied so IGLOO does not overfit its representations to the threshold used for the definition of canonical clusters.

Codebook learning. In addition to learning continuous tokens, the assignment of loops to K discrete tokens offers a convenient and fast approach for loop comparison required for high-throughput queries. For the codebook $C \in \mathbb{R}^{K \times d}$ to learn quantized tokens $\hat{\mathbf{t}}$, we include a codebook learning loss (Van Den Oord et al., 2017) on the classification token of loop u with $\ell_{\text{codebook}, u} = \|\text{sg}[\mathbf{t}_u] - \hat{\mathbf{t}}_u\|_2^2 + \alpha \|\mathbf{t}_u - \text{sg}[\hat{\mathbf{t}}_u]\|_2^2$, where sg is the stop gradient operator and α is the weight on the second commitment loss term.

3.3 TRAINING AND INFERENCE OF IGLOO

For the training of IGLOO we use the overall loss function, which is given by

$$\mathcal{L} = \ell_{\text{dihedral recon.}} + \ell_{\text{AA}} + \ell_{\text{contrastive}} + \ell_{\text{codebook}} + \lambda \ell_{\text{dihedral reg.}} \quad (3)$$

We train IGLOO on heavy and light chain CDR1, CDR2, CDR3, and CDR4 loops from all antibodies and nanobodies in SAbDab (Dunbar et al., 2014), and TCRs in STCRDab (Leem et al., 2018). In addition, we also train with Ibex (Dreyer et al., 2025a) predicted structures of paired heavy and light chain antibodies from paired sequences of the Observed Antibody Space (OAS, Olsen et al. (2022)) (Appendix A.1). For each antibody, we then use their concatenated CDR sequence and an 80% sequence identity threshold for splitting loops of antibodies into train, test, and validation. Since clustering at the level of concatenated sequences of CDRs can still result in an individual CDR sharing the same sequence, any training loop sequences are removed from the validation and test set. In total, IGLOO is trained on 108,167 experimentally resolved loop structures from SAbDab and STCRDab and 699,648 predicted loop structures from paired OAS sequences. At inference, IGLOO outputs a continuous classification loop token \mathbf{t} , a quantized token $\hat{\mathbf{t}}$, and a multimodal representation for each residue i in the loop \mathbf{x}_i .

3.4 INCORPORATING IGLOO TOKENS INTO PROTEIN LANGUAGE MODELS

Approach. We demonstrate how IGLOO loop tokens, \mathbf{t} , can be inserted as special tokens in protein language models with two complementary approaches. (1) IGLOOLM (Fig. 3c) is a protein language model with the IGLOO loop token, \mathbf{t} , inserted at the start of each CDR loop and an `<end>` token added at the end of the loop. (2) IGLOOALM (ALM=dihedral Angle Language Model, Fig. 3d) is a protein language model with the IGLOO loop token, \mathbf{t} , and IGLOO multimodal residue tokens, \mathbf{x}_i , for each amino acid in the CDR loop. These models are finetuned from the 420M parameter base antibody language model, IgBert (Kenlay et al., 2024), a BERT-style model trained on all paired and unpaired OAS sequences. We project IGLOO tokens with a linear layer so that they are the same dimension as the hidden dimension of tokens in the base protein language model.

Learnable classification tokens have been widely used in text, vision, and single-cell transformers (Devlin et al., 2019; Dosovitskiy et al., 2020; Cui et al., 2024). Analogous to the cell-prompting and gene-prompting paradigms of scGPT (Cui et al., 2024), IGLOOLM encodes loops with tokens, \mathbf{t} , while IGLOOALM extends this scheme by combining loop tokens \mathbf{t} and multimodal residue tokens, \mathbf{x} . Embeddings from IGLOOLM contain the context of the loop conformation, while embeddings from IGLOOALM additionally contain the context of the dihedral angles of each residue in the

loop. We demonstrate how IGLOOALM excels in tasks where the accurate residue-level structure is provided. Conversely, IGLOOLM excels in tasks where the loop conformation is known, but accurate residue-level structure prediction is challenging – for example, deep-mutational-scan datasets in which sequences differ by only a few point mutations (Pak et al., 2023; Buel & Walters, 2022).

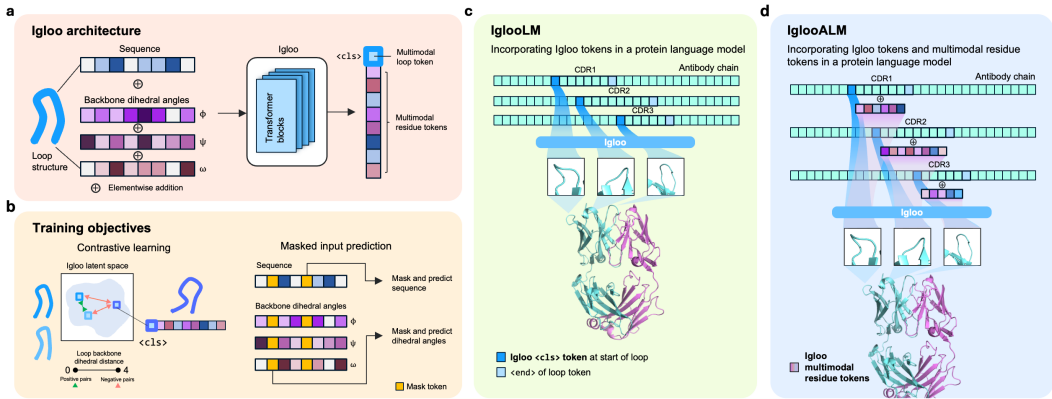


Figure 3: **a** IGLOO is a multimodal tokenizer for antibody loops. **b** Training objectives involve (1) contrastive learning with positive and negative pairs defined by their dihedral angle distance, and (2) masking and prediction of sequence and backbone dihedral angles. How IGLOO tokens of CDR loops can be incorporated into protein language models where **c** IGLOOLM contains only the $\langle c1s \rangle$ (classification) loop token, **t**, and **d** IGLOOALM contains the loop token and multimodal residue tokens.

Training and Inference. The models are finetuned with the same masked language model objective as Kenlay et al. (2024)—uniformly randomly masking 15% of amino acid residues, for which 80% are then replaced by a masked token, 10% are changed to a random token in the vocabulary, and 10% are left unchanged. The same residues are also masked for the computation of the IGLOO token. IGLOOLM and IGLOOALM are trained on single domains from paired OAS sequences, which are split into train, validation, and test splits based on a 90% sequence identity split (Appendix A.2). All structures of the loops required for IGLOO tokens are extracted from Ibx predicted structures.

4 EXPERIMENTS

4.1 IGLOO FOR PARATOPE RETRIEVAL

In this evaluation, for a set of query CDRs, we task IGLOO to retrieve from a large repository of CDRs those with the closest experimentally determined backbone structure, thereby directly assessing how well the representation captures paratope-level structure.

Experimental set up. Query CDRs are from the IGLOO unseen test set of CDRs, and the repository CDRs are those from the train and validation set of SABDab. We use the IGLOO **t** token and retrieve 20 loops with the highest cosine similarity from loops of the same type and length. Retrieved CDRs are deemed correct if $\mathcal{D} < 0.47$ (Eq. 1) or RMSD $< 1 \text{ \AA}$ to the query CDR loop.

Baselines. We compare IGLOO to protein language models that are trained on UniProt: ESM C (ESM Team, 2024) and ESM-2 (3B) (Lin et al., 2023), and models trained on OAS: AbLang2 (Olsen et al., 2024) and IgBert (Kenlay et al., 2024). Additionally, we evaluate the quality of retrieval when structure is also given and compare to multimodal protein language models, SaProt (Su et al., 2023) and ProstT5 (Heinzinger et al., 2024), which also take as input the Foldseek 3Di tokens (Van Kempen et al., 2024) derived from the protein structure. To ensure embeddings focus on the loop, for models which embed the whole protein sequence, the loop embedding is defined as the mean embedding over the amino acids in the loop. We also compare to continuous structure tokenizers which were benchmarked by (Yuan et al., 2025). This includes inverse folding models: MIF (Yang et al., 2023) and ProteinMPNN (Dauparas et al., 2022), and the continuous encoder embedding of VQVAE models: Foldseek 3Di and Amino Aseed (Yuan et al., 2025). For further details see Appendix B.3.

Results. We evaluate the models with precision at rank 20 and observe that IGLOO achieves state-of-the-art performance in retrieving similar paratopes, based on dihedral distance $\mathcal{D} < 0.47$ and RMSD $< 1 \text{ \AA}$ from loops of the same length when given sequence and dihedral angle input (Table 1). Compared to larger protein language models pretrained with masked language modeling, IGLOO and Foldseek achieve higher precision. For the retrieval of similar H3 loop structures based on dihedral distance \mathcal{D} , IGLOO outperforms the best structure tokenizer, Amino Aseed, by 5.9% and the best protein language model or antibody language model, ESM-2 (3B) by 69.8%. The H3 loop is particularly hard to represent for sequence-only language models due to the high sequence diversity owing to V(D)J recombination (Tonegawa, 1983). We also show how ablating key components of the model effects performance in Appendix C.

Table 1: Average precision at rank 20 for retrieval of similar CDR paratopes. Models are shown in rows. The **first**, **second**, and **third** best performance for each column are highlighted. Additional results for precision at rank 1, 5, and 10 are available at Table S4.

Model	L1	L2	% RMSD < 1 Å				% $\mathcal{D} < 0.47$						
			L3	H1	H2	H3	L1	L2	L3	H1	H2	H3	
Random	0.545	0.557	0.373	0.249	0.351	0.127	0.648	0.730	0.392	0.559	0.508	0.126	
PLM	ESM C	0.750	0.700	0.489	0.418	0.519	0.19	0.811	0.916	0.517	0.692	0.702	0.208
	ESM-2 (3B)	0.740	0.704	0.500	0.425	0.522	0.206	0.802	0.904	0.534	0.706	0.688	0.237
AbLM	AbLang2	0.689	0.604	0.482	0.402	0.497	0.173	0.761	0.782	0.537	0.602	0.699	0.222
	IgBert	0.705	0.622	0.482	0.377	0.479	0.182	0.773	0.813	0.511	0.709	0.677	0.216
MPLM	SaProt	0.737	0.704	0.499	0.420	0.491	0.218	0.790	0.918	0.578	0.688	0.646	0.248
	ProstT5	0.782	0.716	0.539	0.458	<u>0.586</u>	0.276	0.846	0.941	<u>0.629</u>	0.711	0.756	0.359
IF	MIF	0.776	0.699	0.516	0.432	0.491	0.231	0.833	0.933	0.604	0.702	0.641	0.298
	ProteinMPNN	<u>0.804</u>	0.700	<u>0.546</u>	<u>0.459</u>	0.521	<u>0.286</u>	0.839	<u>0.943</u>	0.632	0.732	0.710	<u>0.372</u>
VQVAE	Foldseek 3Di	0.785	0.696	<u>0.556</u>	0.467	0.591	<u>0.281</u>	<u>0.849</u>	0.909	<u>0.640</u>	<u>0.715</u>	<u>0.730</u>	0.362
	Amino Aseed	0.812	<u>0.713</u>	0.542	0.420	0.529	0.292	0.851	<u>0.952</u>	0.625	0.688	0.713	<u>0.379</u>
Ours	IGLOO	<u>0.793</u>	<u>0.705</u>	0.558	<u>0.459</u>	<u>0.578</u>	0.278	0.851	0.956	0.674	<u>0.715</u>	<u>0.749</u>	0.402

PLM: Protein Language Model, AbLM: Antibody Language Model, MPLM: Multimodal Protein Language Model, IF: Inverse Folding Model

4.2 IGLOO FOR CLUSTERING ANTIBODY STRUCTURES

The canonical clusters established by North et al. (2011) and Kelow et al. (2022) have been widely used for categorizing new structures (Teplakov et al., 2016) and to analyze molecular dynamics simulations of antibodies (Fernández-Quintero et al., 2020; 2019). In this section, we evaluate how well the quantized token, $\hat{\mathbf{t}}$, recovers their clusters of antibody CDRs.

Evaluation setup. Let the IGLOO learned codebook $\hat{\mathbf{t}}$ induce the partition $\mathcal{C} = \{C_1, \dots, C_K\}$, and let $\mathcal{G} = \{G_1, \dots, G_L\}$ denote the reference clusters of Kelow et al. (2022). We quantify the agreement between these two partitions using *cluster purity*. For each predicted cluster C_k , we select the dominant reference class based on majority vote: $y^*(k) = \arg \max_{\ell} |C_k \cap G_{\ell}|$. Items in C_k whose reference label equals $y^*(k)$ are considered correctly assigned. Overall accuracy is the proportion of correctly assigned instances

$$\text{Purity}(\mathcal{C}, \mathcal{G}) = \frac{1}{N} \sum_{k=1}^K \max_{\ell} |C_k \cap G_{\ell}|, \quad N = \sum_{k=1}^K |C_k|. \quad (4)$$

We evaluate on all loops in SAbDab that can be assigned to a reference cluster with a cutoff of $\mathcal{D} = 0.47$ to the centroid. A limitation of the existing canonical clustering approach is that several loops are not assigned to any cluster. We do not evaluate cluster purity on unassigned loops, which are typically referred to as belonging to “noise” clusters.

The reference definition of clusters assigns different clusters for different loop types and lengths. We also evaluate the cluster’s *loop-type purity* and *loop-length purity* are defined as follows:

$$p_k^{\text{type}} = \frac{1}{n_k} \max_t \sum_{x \in C_k} \mathbb{1}\{\text{loop type}(x) = t\}, \quad p_k^{\text{len}} = \frac{1}{n_k} \max_{\ell} \sum_{x \in C_k} \mathbb{1}\{\text{loop length}(x) = \ell\}, \quad (5)$$

where $t \in \{H1, H2, H3, H4, L1, L2, L3, L4\}$. We report global scores with a weighted average of the cluster-level purity scores, $P^{\text{type}} = \frac{1}{N} \sum_k n_k p_k^{\text{type}}$, $P^{\text{len}} = \frac{1}{N} \sum_k n_k p_k^{\text{len}}$, where n_k is the number of loops in the cluster and $N = \sum_k n_k$.

Results. Across SABDab, 1305 IGLOO codebooks and 180 reference clusters are used. Without exposure to loop-type annotations, the IGLOO-induced partition is highly homogeneous, attaining a loop-type purity of $P^{\text{type}} = 0.983$, and loop length purity $P^{\text{len}} = 0.965$. Visualization of the latent space in 2D with UMAP also shows localization of loops by loop type, length, and canonical cluster (Fig. S1). We report cluster purity in Table 2. Our results are comparable with Wong et al. (2019a) (Table S6), which uses Position-Specific Scoring Matrices to predict canonical forms from sequence. These results highlight IGLOO can recover the known canonical clusters with high purity.

We further explore how different loops differ in their distribution across codebooks. The proportion of each loop in SABDab assigned to the top 20 used codebooks is shown in Fig. 4 for each loop type. The H4 and L2 loop types have relatively low diversity with 93.0% and 91.7% of loops assigned to a codebook in the top 20, respectively. Conversely, H3 has the lowest coverage in the top 20 codebooks with 14.6% of loops. The most frequent H3-loop codebook entry appears 387 times. Every occurrence shares an identical loop sequence derived from single-chain Fv16 antibody structures, a scaffold that is widely represented in the PDB.

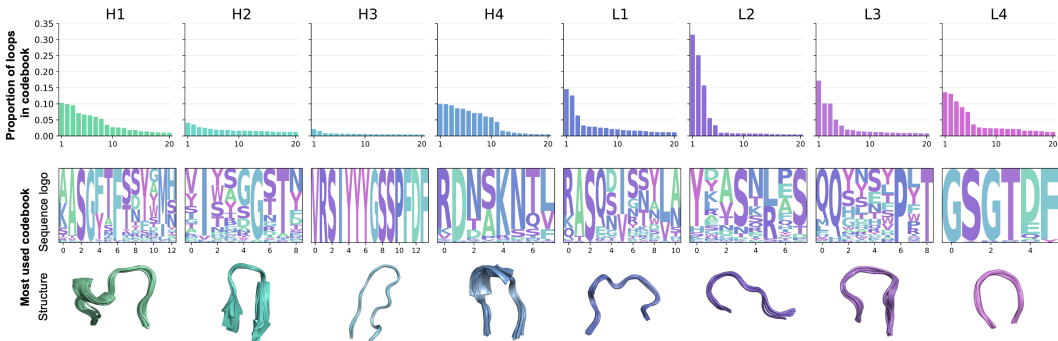


Figure 4: **Top** Top 20 used IGLOO codebooks for each CDR type in SABDab. **Bottom** Sequence logo and aligned structures of 20 loops for the most used IGLOO codebook for each loop type.

4.3 PREDICTING BINDING AFFINITY WITH IGLOOLM

Next, IGLOOLM is evaluated on datasets where sequences differ by a few variants. For a set of heavy chain antibody mutants, we apply the protein-level representations of the heavy chain sequences to predict binding affinity. This section aims to test if incorporating IGLOO tokens, t , into protein language models as a special token is beneficial to the representations learned by the model.

Experimental setup. We use the curated set of antibody-antigen binding affinity dataset from Ab-BiBench (Zhao et al., 2025a). Antibody structures for the variants are predicted with Ibex, used as input to obtain IGLOO tokens, and embeddings are then generated with IGLOOLM. Sequence-level embeddings are obtained by averaging residue-level embeddings. A separate model is trained for each antibody-antigen pair. Sequence-level embeddings are used as input to train a ridge regressor evaluated with 10-fold nested cross-validation (Appendix B.4). Models are evaluated with the Spearman correlation coefficient, ρ , between the predicted and true binding affinity.

Baselines. The protein language models, ESM C, ESM-2 (3B), AbLang2, and IgBert, and multi-modal protein language models SaProt and ProstT5 introduced in Section 4.1 are used as baselines. We obtain sequence-level embeddings by averaging the residue-level embeddings. For the multi-modal protein language models, we use Foldseek 3Di tokens from the Ibex predicted structures.

Results. Across the 10 antibody-antigen pairs in Table 3, IGLOOLM surpasses the base model IgBert from which it is derived on 8 cases. It ranks first or second on 7 of the 10 pairs. The results also show that structure is not always beneficial, with the structure-only protein language model, ProstT5, which uses the Foldseek 3Di alphabet, and the sequence-structure protein language model, SaProt, not performing as well as sequence-only models. Comparing IGLOOLM and IGLOOLM

(Table S7), which is given all dihedral angle input rather than a summarized classification token, we also see a drop in performance. Therefore, showing the benefit of incorporating only the IGLOO classification token into IGLOOLM for representing proteins which differ by a few mutations. As protein language models improve with scale (Lin et al., 2023), it is notable that IGLOOLM, a 420M parameter model more than $7\times$ smaller than ESM-2 (3B), achieves better performance on average across the 10 antibody-antigens.

Table 3: Spearman correlation coefficient (\uparrow) for binding affinity prediction across 10 different targets from AbBiBench. The **first** and **second** values are highlighted. We report the standard error across the 10 fold cross-validation in parentheses.

Target	ESM C	ESM-2 (3B)	SaProt	ProstT5	AbLang2	IgBert	IGLOOLM
1mlc	0.609 (0.017)	0.551 (0.013)	0.557 (0.020)	0.280 (0.040)	0.634 (0.015)	0.665 (0.015)	0.616 (0.009)
1n8z	0.673 (0.022)	0.635 (0.019)	0.637 (0.028)	0.351 (0.057)	0.646 (0.021)	0.682 (0.023)	0.675 (0.025)
2fxg	0.809 (0.010)	0.752 (0.010)	0.754 (0.012)	0.355 (0.021)	0.752 (0.007)	0.694 (0.013)	0.713 (0.014)
3gbn_h1	0.901 (0.004)	0.953 (0.003)	0.915 (0.005)	0.638 (0.013)	0.945 (0.004)	0.947 (0.004)	0.948 (0.004)
3gbn_h9	0.932 (0.004)	0.971 (0.002)	0.952 (0.003)	0.679 (0.017)	0.963 (0.003)	0.961 (0.003)	0.962 (0.003)
4fqi_h1	0.871 (0.001)	0.955 (0.001)	0.866 (0.001)	0.593 (0.002)	0.883 (0.001)	0.898 (0.001)	0.921 (0.001)
4fqi_h3	0.936 (0.001)	0.973 (0.001)	0.958 (0.001)	0.644 (0.009)	0.969 (0.001)	0.970 (0.001)	0.971 (0.001)
aay149	0.617 (0.010)	0.584 (0.013)	0.584 (0.012)	0.301 (0.014)	0.563 (0.010)	0.611 (0.010)	0.625 (0.010)
aay149_ML	0.518 (0.008)	0.524 (0.008)	0.487 (0.009)	0.320 (0.009)	0.499 (0.007)	0.524 (0.007)	0.531 (0.007)
aay151	0.576 (0.007)	0.516 (0.009)	0.524 (0.008)	0.260 (0.011)	0.527 (0.009)	0.566 (0.010)	0.579 (0.011)

4.4 CONTROLLABLE SAMPLING OF ANTIBODY LOOPS

In this section, we evaluate IGLOOLM on its ability to guide the structure of the loop at the residue level, by analyzing if sampled loops are consistent in structure to the masked out loop.

Experiment setup. For the CDR1, CDR2, and CDR3 of the heavy and light chain, we randomly sample 50 structures from SABDab, which are in the test set of IGLOO. IGLOO t, X tokens of the dihedral angles and masked sequence are inputted to IGLOOLM. We sample loop sequences from the resulting amino acid likelihoods of IGLOOLM for each of these antibodies and fold the sampled sequence with Ibx.

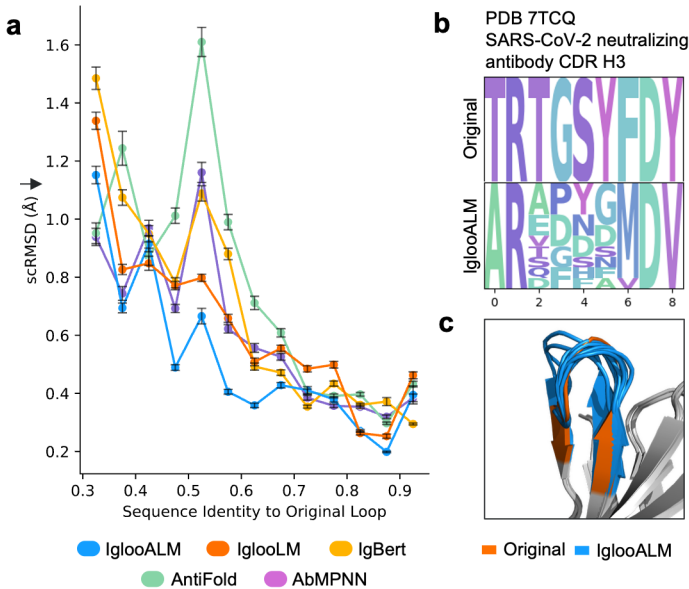


Figure 5: **a** Mean self-consistency (sc) RMSD (\AA) \downarrow of sampled loop sequences compared to original loop structures across sequence identity bins. Error bars show standard error of the mean across the generated structures aggregated in each sequence identity bin. **b** Sequence logo of original and ten IGLOOLM sampled sequences of the CDR H3 loop region for a SARS-CoV-2 neutralizing antibody (PDB 7TCQ) at $\lambda = 0.5$. **c** Predicted structure of the CDR H3 loop regions aligned to PDB 7TCQ.

Results. We show the scRMSD of the sampled loops stratified by sequence identity (Fig. 5a). IGLOOALM excels at generating loops at different levels of sequence diversity while maintaining a similar structure, improving both on state-of-the-art antibody inverse folding models and the base model. We highlight a particular example for the redesign of the H3 loop of a SARS-CoV-2 neutralizing antibody from the PDB structure 7TCQ. At a sampling temperature of 0.5, IGLOOALM samples loops with an average edit distance of 6.6 from the loop of length 9 (Fig. 5b). The predicted structures of the sampled loops maintain the beta hairpin structure of the original loop with an average loop RMSD of 0.79 Å (Fig. 5c). Other examples of sampled loops and their structures are presented in Fig. S2.

Baselines. We evaluate against recently published state-of-the-art inverse folding models for antibodies: AbMPNN (Dreyer et al., 2023)—a version of ProteinMPNN (Dauparas et al., 2022) finetuned on antibody structures, and AntiFold (Høie et al., 2024)—a version of ESM-IF1 (Hsu et al., 2022) finetuned on antibody structures. For these models, we only generate the loop sequence given the full backbone and the sequence of the rest of the antibody. We also compare to the base model, IgBert, and IGLOOLM which does not include the multimodal residue tokens x .

Evaluation setup. For each loop and model, we sample 10 sequences at the following sampling temperatures: $\lambda = 0.01, 0.05, 0.1, 0.2, 0.5, 1.0, 2.0$. In total, for each model, we generate $50 \times 10 \times 6 \times 7 = 21,000$ sequences for the different structures, sequence samples, loop types, and temperatures, respectively. Then we align the generated loop regions with the original structure and evaluate the self-consistency (sc) RMSD between the two loop structures. Sampling sequences at different temperatures is necessary to generate sequences with different levels of sequence identity to the original loop, since recapitulating the original loop sequence would achieve low scRMSD but would not be useful for the design of new H3 loops.

5 CONCLUSION

Here we present IGLOO, a multimodal tokenizer for antibody loops with a novel contrastive learning objective based on dihedral angle distance between loop backbones. Applying IGLOO, we achieve state-of-the-art results in retrieving similar loop conformations and recover known canonical clusters. IGLOO tokens can also be incorporated into protein language models for improved binding affinity predictions with IGLOOLM and for controllable generation of antibody loops with IGLOOALM. While IGLOOALM demonstrates strong *in silico* results, more comprehensive wet-lab validation evaluation is needed to evaluate whether redesigned antibodies maintain binding with antigens. IGLOO could be further extended to incorporate other modalities such as all-atom structure, epitope information, function, and binding affinity. We also envision IGLOO could be applied to lead optimization and affinity maturation of antibodies (Makowski et al., 2022; Dreyer et al., 2025b; Frey et al., 2025). By introducing multimodal loop tokens, IGLOO opens new directions for multimodal foundation models for rational antibody design.

ACKNOWLEDGMENTS

We are grateful to Joshua Southern, Sidney Lisanza, Nathan Frey, Saeed Saremi, Sarah Robinson, Imee Sinha, Catherine Wong, Pan Kessel, Leon Hetzel, Franziska Seeger, and the rest of the Prescient Design team for useful discussions.

REPRODUCIBILITY STATEMENT

All code for data processing, implementation, training scripts, evaluation and analyses scripts, and for reproducing results in the paper is available at <https://github.com/prescient-design/igloo>. Details of the dataset used for training IGLOO are provided in Appendix A.1, and for training IGLOOLM and IGLOOALM are provided in Appendix A.2. Details for processing of AbBiBench data are available at Appendix A.3. Training details, hyperparameters, GPUs used, and training duration for training IGLOO, IGLOOLM, IGLOOALM, and regression models for AbBiBench are available at Appendix B. The transformer architecture used in IGLOO is based on the `TransformerLayer` from ESM-2 available at <https://github.com/facebookresearch/esm>. The base model, IgBert (Kenlay et al., 2024),

is publicly available at <https://huggingface.co/Exscientia/IgBert>. Code for fine-tuning IgBert for IGLOOLM and IGLOOALM is available on our GitHub. Full details of the IGLOO loss function and objective are available at Section 3.2. All evaluation metrics used for experiments are specified explicitly in Section 4.

ETHICS STATEMENT

IGLOO is a method for tokenizing loop regions of antibodies and may be used for antibody design. All antibody sequences used to develop and evaluate IGLOO were obtained from publicly available databases and contain no personal or patient-identifiable information. No new animal or human subjects were involved. Methods that facilitate antibody engineering can present dual-use concerns. Here we present use cases where IGLOO is applied for achieving positive impact.

REFERENCES

- Jared Adolf-Bryfogle, Qifang Xu, Benjamin North, Andreas Lehmann, and Roland L Dunbrack Jr. Pyigclassify: a database of antibody cdr structural classifications. *Nucleic acids research*, 43(D1): D432–D438, 2015.
- Jared Adolf-Bryfogle, Oleks Kalyuzhnyi, Michael Kubitz, Brian D Weitzner, Xiaozhen Hu, Yumiko Adachi, William R Schief, and Roland L Dunbrack Jr. Rosettaantibodydesign (rabd): A general framework for computational antibody design. *PLoS computational biology*, 14(4):e1006112, 2018.
- Gwen R Buel and Kylie J Walters. Can alphafold2 predict the impact of missense mutations on structure? *Nature structural & molecular biology*, 29(1):1–2, 2022.
- Cyrus Chothia and Arthur M Lesk. Canonical structures for the hypervariable regions of immunoglobulins. *Journal of molecular biology*, 196(4):901–917, 1987.
- Silvia Crescioli, H el ene Kaplon, Lin Wang, Jyothsna Visweswaraiah, Vaishali Kapoor, and Janice M Reichert. Antibodies to watch in 2025. In *MAbs*, volume 17, pp. 2443538. Taylor & Francis, 2025.
- Haotian Cui, Chloe Wang, Hassaan Maan, Kuan Pang, Fengning Luo, Nan Duan, and Bo Wang. scgpt: toward building a foundation model for single-cell multi-omics using generative ai. *Nature methods*, 21(8):1470–1480, 2024.
- Justas Dauparas, Ivan Anishchenko, Nathaniel Bennett, Hua Bai, Robert J Ragotte, Lukas F Milles, Basile IM Wicky, Alexis Courbet, Rob J de Haas, Neville Bethel, et al. Robust deep learning-based protein sequence design using proteinmpnn. *Science*, 378(6615):49–56, 2022.
- Jacob Devlin, Ming-Wei Chang, Kenton Lee, and Kristina Toutanova. Bert: Pre-training of deep bidirectional transformers for language understanding. In *Proceedings of the 2019 conference of the North American chapter of the association for computational linguistics: human language technologies, volume 1 (long and short papers)*, pp. 4171–4186, 2019.
- Alexey Dosovitskiy, Lucas Beyer, Alexander Kolesnikov, Dirk Weissenborn, Xiaohua Zhai, Thomas Unterthiner, Mostafa Dehghani, Matthias Minderer, Georg Heigold, Sylvain Gelly, et al. An image is worth 16x16 words: Transformers for image recognition at scale. *arXiv preprint arXiv:2010.11929*, 2020.
- Fr ed eric A Dreyer, Daniel Cutting, Constantin Schneider, Henry Kenlay, and Charlotte M Deane. Inverse folding for antibody sequence design using deep learning. *arXiv preprint arXiv:2310.19513*, 2023.
- Fr ed eric A Dreyer, Jan Ludwiczak, Karolis Martinkus, Brennan Abanades, Robert G Alberstein, Pan Kessel, Pranav Rao, Jae Hyeon Lee, Richard Bonneau, Andrew M Watkins, et al. Conformation-aware structure prediction of antigen-recognizing immune proteins. *arXiv preprint arXiv:2507.09054*, 2025a.

-
- Frédéric A Dreyer, Constantin Schneider, Aleksandr Kovaltsuk, Daniel Cutting, Matthew J Byrne, Daniel A Nissley, Henry Kenlay, Claire Marks, David Errington, Richard J Gildea, et al. Computational design of therapeutic antibodies with improved developability: efficient traversal of binder landscapes and rescue of escape mutations. In *mAbs*, volume 17, pp. 2511220. Taylor & Francis, 2025b.
- James Dunbar and Charlotte M Deane. Anarci: antigen receptor numbering and receptor classification. *Bioinformatics*, 32(2):298–300, 2016.
- James Dunbar, Konrad Krawczyk, Jinwoo Leem, Terry Baker, Angelika Fuchs, Guy Georges, Jiye Shi, and Charlotte M Deane. Sabdad: the structural antibody database. *Nucleic acids research*, 42(D1):D1140–D1146, 2014.
- ESM Team. Esm cambrian: Revealing the mysteries of proteins with unsupervised learning, December 2024. URL <https://evolutionaryscale.ai/blog/esm-cambrian>.
- Ada Fang, Michael Desgagné, Zaixi Zhang, Andrew Zhou, Joseph Loscalzo, Bradley L Pentelute, and Marinka Zitnik. Learning universal representations of intermolecular interactions with atomica. In *Review*, 2025. URL <https://www.biorxiv.org/content/10.1101/2025.04.02.646906>.
- Monica L Fernández-Quintero, Barbara A Math, Johannes R Loeffler, and Klaus R Liedl. Transitions of cdr-13 loop canonical cluster conformations on the micro-to-millisecond timescale. *Frontiers in immunology*, 10:2652, 2019.
- Monica L Fernández-Quintero, Martin C Heiss, Nancy D Pomarici, Barbara A Math, and Klaus R Liedl. Antibody cdr loops as ensembles in solution vs. canonical clusters from x-ray structures. In *MAbs*, volume 12, pp. 1744328. Taylor & Francis, 2020.
- Nathan C Frey, Isidro Hötzel, Samuel D Stanton, Ryan Kelly, Robert G Alberstein, Emily Makowski, Karolis Martinkus, Daniel Berenberg, Jack Bevers III, Tyler Bryson, et al. Lab-in-the-loop therapeutic antibody design with deep learning. *bioRxiv*, pp. 2025–02, 2025.
- Toni Giorgino. Computing and visualizing dynamic time warping alignments in r: the dtw package. *Journal of statistical Software*, 31:1–24, 2009.
- Thomas Hayes, Roshan Rao, Halil Akin, Nicholas J Sofroniew, Deniz Oktay, Zeming Lin, Robert Verkuil, Vincent Q Tran, Jonathan Deaton, Marius Wiggert, et al. Simulating 500 million years of evolution with a language model. *Science*, pp. eads0018, 2025.
- Michael Heinzinger, Konstantin Weissenow, Joaquin Gomez Sanchez, Adrian Henkel, Milot Mirdita, Martin Steinegger, and Burkhard Rost. Bilingual language model for protein sequence and structure. *NAR Genomics and Bioinformatics*, 6(4):lqae150, 2024.
- Brian L Hie, Varun R Shanker, Duo Xu, Theodora UJ Bruun, Payton A Weidenbacher, Shaogeng Tang, Wesley Wu, John E Pak, and Peter S Kim. Efficient evolution of human antibodies from general protein language models. *Nature biotechnology*, 42(2):275–283, 2024.
- Magnus Haraldson Høie, Alissa Hummer, Tobias H Olsen, Broncio Aguilar-Sanjuan, Morten Nielsen, and Charlotte M Deane. Antifold: Improved antibody structure-based design using inverse folding. *arXiv preprint arXiv:2405.03370*, 2024.
- Annemarie Honegger and Andreas Pluëckthun. Yet another numbering scheme for immunoglobulin variable domains: an automatic modeling and analysis tool. *Journal of molecular biology*, 309(3):657–670, 2001.
- Chloe Hsu, Robert Verkuil, Jason Liu, Zeming Lin, Brian Hie, Tom Sercu, Adam Lerer, and Alexander Rives. Learning inverse folding from millions of predicted structures. In *International conference on machine learning*, pp. 8946–8970. PMLR, 2022.
- Bowen Jing, Stephan Eismann, Patricia Suriana, Raphael JL Townshend, and Ron Dror. Learning from protein structure with geometric vector perceptrons. *arXiv preprint arXiv:2009.01411*, 2020.

-
- Simon Kelow, Bulat Faezov, Qifang Xu, Mitchell Parker, Jared Adolf-Bryfogle, and Roland L Dunbrack Jr. A penultimate classification of canonical antibody cdr conformations. *bioRxiv*, pp. 2022–10, 2022.
- Simon P Kelow, Jared Adolf-Bryfogle, and Roland L Dunbrack. Hiding in plain sight: structure and sequence analysis reveals the importance of the antibody de loop for antibody-antigen binding. In *MAbs*, volume 12, pp. 1840005. Taylor & Francis, 2020.
- Henry Kenlay, Frédéric A Dreyer, Aleksandr Kovaltsuk, Dom Miketa, Douglas Pires, and Charlotte M Deane. Large scale paired antibody language models. *PLOS Computational Biology*, 20(12):e1012646, 2024.
- Maxat Kulmanov, Francisco J Guzmán-Vega, Paula Duek Roggli, Lydie Lane, Stefan T Arold, and Robert Hoehndorf. Protein function prediction as approximate semantic entailment. *Nature Machine Intelligence*, 6(2):220–228, 2024.
- Jinwoo Leem, Saulo H P de Oliveira, Konrad Krawczyk, and Charlotte M Deane. Stcrdab: the structural t-cell receptor database. *Nucleic acids research*, 46(D1):D406–D412, 2018.
- Mingchen Li, Yang Tan, Xinzhu Ma, Bozitao Zhong, Huiqun Yu, Ziyi Zhou, Wanli Ouyang, Bingxin Zhou, Pan Tan, and Liang Hong. Prosst: Protein language modeling with quantized structure and disentangled attention. *Advances in Neural Information Processing Systems*, 37:35700–35726, 2024.
- Zeming Lin, Halil Akin, Roshan Rao, Brian Hie, Zhongkai Zhu, Wenting Lu, Nikita Smetanin, Robert Verkuil, Ori Kabeli, Yaniv Shmueli, et al. Evolutionary-scale prediction of atomic-level protein structure with a language model. *Science*, 379(6637):1123–1130, 2023.
- Chu’nan Liu, Lilian M Denzler, Oliver EC Hood, and Andrew CR Martin. Do antibody cdr loops change conformation upon binding? In *MAbs*, volume 16, pp. 2322533. Taylor & Francis, 2024.
- Loredana Lo Conte, Bart Ailey, Tim JP Hubbard, Steven E Brenner, Alexey G Murzin, and Cyrus Chothia. Scop: a structural classification of proteins database. *Nucleic acids research*, 28(1): 257–259, 2000.
- Emily K Makowski, Patrick C Kinnunen, Jie Huang, Lina Wu, Matthew D Smith, Tiexin Wang, Alec A Desai, Craig N Streu, Yulei Zhang, Jennifer M Zupancic, et al. Co-optimization of therapeutic antibody affinity and specificity using machine learning models that generalize to novel mutational space. *Nature communications*, 13(1):3788, 2022.
- Leland McInnes, John Healy, and James Melville. Umap: Uniform manifold approximation and projection for dimension reduction. *arXiv preprint arXiv:1802.03426*, 2018.
- Jaina Mistry, Sara Chuguransky, Lowri Williams, Matloob Qureshi, Gustavo A Salazar, Erik LL Sonnhammer, Silvio CE Tosatto, Lisanna Paladin, Shriya Raj, Lorna J Richardson, et al. Pfam: The protein families database in 2021. *Nucleic acids research*, 49(D1):D412–D419, 2021.
- Benjamin North, Andreas Lehmann, and Roland L Dunbrack Jr. A new clustering of antibody cdr loop conformations. *Journal of molecular biology*, 406(2):228–256, 2011.
- Pascal Notin, Aaron Kollasch, Daniel Ritter, Lood Van Niekerk, Steffanie Paul, Han Spinner, Nathan Rollins, Ada Shaw, Rose Orenbuch, Ruben Weitzman, et al. Proteingym: Large-scale benchmarks for protein fitness prediction and design. *Advances in Neural Information Processing Systems*, 36: 64331–64379, 2023.
- Jaroslav Nowak, Terry Baker, Guy Georges, Sebastian Kelm, Stefan Klostermann, Jiye Shi, Sudharsan Sridharan, and Charlotte M Deane. Length-independent structural similarities enrich the antibody cdr canonical class model. In *MAbs*, volume 8, pp. 751–760. Taylor & Francis, 2016.
- Tobias H Olsen, Fergus Boyles, and Charlotte M Deane. Observed antibody space: A diverse database of cleaned, annotated, and translated unpaired and paired antibody sequences. *Protein Science*, 31(1):141–146, 2022.

-
- Tobias H Olsen, Iain H Moal, and Charlotte M Deane. Addressing the antibody germline bias and its effect on language models for improved antibody design. *Bioinformatics*, 40(11):btae618, 2024.
- Christos A Ouzounis, Richard MR Coulson, Anton J Enright, Victor Kunin, and José B Pereira-Leal. Classification schemes for protein structure and function. *Nature Reviews Genetics*, 4(7): 508–519, 2003.
- Marina A Pak, Karina A Markhieva, Mariia S Novikova, Dmitry S Petrov, Ilya S Vorobyev, Ekaterina S Maksimova, Fyodor A Kondrashov, and Dmitry N Ivankov. Using alphafold to predict the impact of single mutations on protein stability and function. *Plos one*, 18(3):e0282689, 2023.
- Dario Pavllo, David Grangier, and Michael Auli. Quaternet: A quaternion-based recurrent model for human motion. *arXiv preprint arXiv:1805.06485*, 2018.
- Hiroki Shirai, Akinori Kidera, and Haruki Nakamura. Structural classification of cdr-h3 in antibodies. *FEBS letters*, 399(1-2):1–8, 1996.
- Christian JA Sigrist, Lorenzo Cerutti, Edouard De Castro, Petra S Langendijk-Genevaux, Virginie Bulliard, Amos Bairoch, and Nicolas Hulo. Prosite, a protein domain database for functional characterization and annotation. *Nucleic acids research*, 38(suppl_1):D161–D166, 2010.
- Martin Steinegger and Johannes Söding. Mmseqs2 enables sensitive protein sequence searching for the analysis of massive data sets. *Nature biotechnology*, 35(11):1026–1028, 2017.
- Jin Su, Chenchen Han, Yuyang Zhou, Junjie Shan, Xibin Zhou, and Fajie Yuan. Saprot: Protein language modeling with structure-aware vocabulary. *bioRxiv*, pp. 2023–10, 2023.
- Yang Tan, Bingxin Zhou, Lirong Zheng, Guisheng Fan, and Liang Hong. Semantical and geometrical protein encoding toward enhanced bioactivity and thermostability. *Elife*, 13:RP98033, 2025.
- Alexey Teplyakov, Galina Obmolova, Thomas J Malia, Jinquan Luo, Salman Muzammil, Raymond Sweet, Juan Carlos Almagro, and Gary L Gilliland. Structural diversity in a human antibody germline library. In *MABs*, volume 8, pp. 1045–1063. Taylor & Francis, 2016.
- Susumu Tonegawa. Somatic generation of antibody diversity. *Nature*, 302(5909):575–581, 1983.
- Aaron Van Den Oord, Oriol Vinyals, et al. Neural discrete representation learning. *Advances in neural information processing systems*, 30, 2017.
- Michel Van Kempen, Stephanie S Kim, Charlotte Tumescheit, Milot Mirdita, Jeongjae Lee, Cameron LM Gilchrist, Johannes Söding, and Martin Steinegger. Fast and accurate protein structure search with foldseek. *Nature biotechnology*, 42(2):243–246, 2024.
- Limei Wang, Haoran Liu, Yi Liu, Jerry Kurtin, and Shuiwang Ji. Learning hierarchical protein representations via complete 3d graph networks. *arXiv preprint arXiv:2207.12600*, 2022.
- Wing Ki Wong, Guy Georges, Francesca Ros, Sebastian Kelm, Alan P Lewis, Bruck Taddese, Jinwoo Leem, and Charlotte M Deane. Scalop: sequence-based antibody canonical loop structure annotation. *Bioinformatics*, 35(10):1774–1776, 2019a.
- Wing Ki Wong, Jinwoo Leem, and Charlotte M Deane. Comparative analysis of the cdr loops of antigen receptors. *Frontiers in immunology*, 10:2454, 2019b.
- John L Xu and Mark M Davis. Diversity in the cdr3 region of vh is sufficient for most antibody specificities. *Immunity*, 13(1):37–45, 2000.
- Kevin K Yang, Niccolò Zanichelli, and Hugh Yeh. Masked inverse folding with sequence transfer for protein representation learning. *Protein Engineering, Design and Selection*, 36:gza015, 2023.
- Xinyu Yuan, Zichen Wang, Marcus Collins, and Huzefa Rangwala. Protein structure tokenization: Benchmarking and new recipe. *arXiv preprint arXiv:2503.00089*, 2025.

Xingyi Zhang, Kun Xie, Ningqiao Huang, Wei Liu, Peilin Zhao, Sibao Wang, Kangfei Zhao, and Biaobin Jiang. Fast and accurate antibody sequence design via structure retrieval. *arXiv preprint arXiv:2502.19395*, 2025.

Zuobai Zhang, Minghao Xu, Arian Jamasb, Vijil Chenthamarakshan, Aurelie Lozano, Payel Das, and Jian Tang. Protein representation learning by geometric structure pretraining. *arXiv preprint arXiv:2203.06125*, 2022.

Xinyan Zhao, Yi-Ching Tang, Akshita Singh, Victor J Cantu, KwanHo An, Junseok Lee, Adam E Stogsdill, Ashwin Kumar Ramesh, Zhiqiang An, Xiaoqian Jiang, et al. Benchmark for antibody binding affinity maturation and design. *arXiv preprint arXiv:2506.04235*, 2025a.

Xinyan Zhao, Yi-Ching Tang, Akshita Singh, Victor J Cantu, KwanHo An, Junseok Lee, Adam E Stogsdill, Ashwin Kumar Ramesh, Zhiqiang An, Xiaoqian Jiang, et al. Benchmark for antibody binding affinity maturation and design. *arXiv preprint arXiv:2506.04235*, 2025b.

A DATASET PROCESSING

A.1 IGLOO TRAINING DATA

We process 18,303 structures from SAbDab and STCRDab, which are comprised of 14,341 antibodies, 3,095 nanobodies, and 867 TCRs. From these structures, we run ANARCI (Dunbar & Deane, 2016) on the sequences to identify the loop regions (CDR1, CDR2, CDR3, CDR4) in the North definition North et al. (2011) from their AHO alignment (Honegger & Pluëckthun, 2001). A valid loop requires defined ϕ, ψ, ω angles and at least 5 residues before and after the loop, referred to as the stem region, yielding 108,167 loop structures. To define a train, test, and validation split, we cluster on the concatenated CDR sequences with MMseqs2 (Steinegger & Söding, 2017), using an 80% sequence identity threshold.

Ibex (Dreyer et al., 2025a) predicted CDR loops from antibodies in paired OAS are also included in the IGLOO training set. To maximize sequence diversity of the predicted loop structures, they are downsampled from an initial set of 2,447,258 down to 87,456 by clustering on both concatenated CDR sequences as well as H3 loop sequences with MMseqs2 (Steinegger & Söding, 2017), using a 50% sequence identity threshold. In total, we include 699,648 predicted loop structures in the training set.

Table S1: Number of each loop type in the IGLOO training dataset from SAbDab, STCRDab and paired OAS.

Loop Type	SAbDab and STCRDab	Paired OAS
H1	14,877	87,456
H2	14,876	87,456
H3	14,875	87,456
H4	14,877	87,456
L1	12,167	87,456
L2	12,168	87,456
L3	12,159	87,456
L4	12,168	87,456
Total	108,167	699,648

A.2 IGLOOLM AND IGLOOALM TRAINING DATA

We fold the heavy and light chain with Ibex for 2,447,258 antibodies. The heavy chains and light chains are clustered separately with MMseqs2 (Steinegger & Söding, 2017), using a 90% sequence identity threshold. This results in 247,156 light chain clusters and 875,767 heavy chain clusters. We randomly sample 10,000 light chain and 20,000 heavy chain clusters for the validation and test sets, respectively. For the training set, we keep all sequences in the sequence identity clusters, and for

the validation and test sets, we only keep the representative sequence from each cluster. In total, we train IGLOOLM and IGLOOALM on 4,598,332 antibody chains.

A.3 ABBIBENCH DATA

We use AbBiBench (Zhao et al., 2025a) benchmark, which has for an antibody-antigen pair, heavy chain mutant sequences and their binding affinity score. The binding affinity score is the $-\log K_d$ for all antibody-antigen pairs except for 2fjg and 1mlc, which is log enrichment. For some antibody-antigens, we filter out sequences that do not have binding affinity scores and are given default scores instead. The final number of sequences and filtered used for each antibody-antigen target is shown in Table S2. We train models for 10 out of 11 antibody-antigens in AbBiBench. The Integrin- α -1 AQC2 antibody-antigen dataset is not tested due to an insufficient number of binding affinity measurements ($N = 40$). For each sequence, we fold the heavy chain with the light chain from the structure in the PDB ID with Ibex and extract the structures of the loops for IGLOOLM. All binding affinity values for an antibody-antigen pair are scaled by subtracting the mean of the training distribution and scaling to unit variance.

Table S2: Number of sequences for each antibody-antigen in the AbBiBench benchmarking dataset.

PDB ID	Seed antibody	Antigen	Number of sequences	Filtered out values
1n8z	Trastuzumab	HER2	419	-
1mlc	D44.1	Hen-egg-white lysozyme	1,229	-
2fjg	G6.31	VEGF	2,223	-
3gbn_h1	CR6261	Influenza A/New Caledonia/20/99 (H1N1)	1,673	7.0
3gbn_h9	CR6261	Influenza A/Hong Kong/1073/1999 (H9N2)	1,470	7.0
4fqj_h1	CR9114	Influenza A/New Caledonia/20/99 (H1N1)	63,419	7.0
4fqj_h3	CR9114	Influenza A/Wisconsin/67/2005 (H3N2)	7,174	6.0
aayl49	AAYL49	Spike HR2	4,312	-
aayl49_ML	AAYL49_ML	Spike HR2	8,953	-
aayl51	AAYL51	Spike HR2	4,320	-

B IMPLEMENTATION DETAILS

B.1 TRAINING IGLOO

IGLOO is trained for 100 epochs on 1 NVIDIA H100. We set the following hyperparameters for training IGLOO to be dihedral temperature (0.1), unit circle regularization weight (0.01), number of transformer layers (4), codebook commit loss weight (0.5), max loop length (36), and batch size (64). The following hyperparameters were chosen from: learning rate ($10^{-5} - 10^{-3}$), embedding dimension (32, 128, 1024), codebook size (1024, 8192), and weight decay (0, 10^{-5}). We select the checkpoint at the epoch with the lowest validation loss and select the best hyperparameter based on the average recovery of the canonical clusters (Kelow et al., 2022) on the validation set. We use a two-phase training approach; in the first phase, the model is trained on the SAbDab and paired OAS dataset, and in the second phase, the model is trained only on SAbDab. We use an embedding dimension of 128 and a codebook size of 8192. In the first stage, the learning rate is 5×10^{-5} and weight decay 0, and for the second stage, a learning rate of 5×10^{-5} and weight decay of 10^{-5} is used.

B.2 TRAINING IGLOOLM AND IGLOOALM

We take the publicly available pretrained weights and hyperparameters from IgBert (Kenlay et al., 2024) and continue to finetune the model with the IGLOO tokens for IGLOOLM, and with IGLOO tokens and multimodal residue tokens for IGLOOALM. Both models were trained for 3 days on 4 NVIDIA H100s, which correspond to 53k steps over 5 epochs.

B.3 PARATOPE RETRIEVAL

For obtaining embeddings from the baseline models ESM C, ESM-2 (3B), AbLang2, IgBert, ProstT5, AbLang2, and IgBert, we use publicly available weights and embed the whole antibody

chain and use the mean embedding of the loop residues as the loop embedding. For the structure tokenizers MIF, ProteinMPNN, and Amino Aseed (continuous tokens) we use the implementation provided by (Yuan et al., 2025) and average residue-level tokens over the loop region to obtain a loop embedding. For Foldseek 3Di, since the embeddings are only 2-dimensional, we concatenate the flattened representations of all of the residues in the loop region to obtain the loop embedding.

B.4 TRAINING REGRESSION MODELS FOR ABBIBENCH

For the embeddings of each model and antibody-antigen target, we train a ridge regression with a 10-fold nested cross-validation. The 10 outer folds are used for testing, each containing a 5-fold inner cross-validation that selects the optimal L2 penalty $\lambda \in \{1, 10^{-1}, 10^{-2}, \dots, 10^{-6}, 0\}$ within that fold. For every outer fold, the model was retrained with its fold-specific best λ on the entire training partition, scored on the held-out test partition, and the Spearman correlation coefficient, ρ , is averaged across the 10 folds.

C ABLATION STUDY

To evaluate the contributions of the components of IGLOO, we conduct the following ablation studies to understand the effect of (1) the dihedral distance contrastive loss, (2) distance-threshold filtering of positive ($\mathcal{D} < 0.1$) and negative ($\mathcal{D} > 0.47$) pairs, (3) the sequence modality track, (4) the dihedral angle modality track, and (5) only defining positive pairs between loops of the same length (Appendix D). We evaluate the ablated models with the same experimental setup as outlined in Section 4.1.

Table S3: Average precision at rank 1, 5, 10, and 20 for retrieval of similar CDR paratopes evaluated with $\text{RMSD} < 1\text{\AA}$ and $\mathcal{D} < 0.47$. The **first** and **second** best performance are highlighted below. CL is contrastive learning, DT filter is distance-threshold filter of positive ($\mathcal{D} < 0.1$) and negative ($\mathcal{D} > 0.47$) pairs, and loop length refers to training IGLOO with positive pairs defined between loops of different lengths (Appendix D).

# Loops retrieved	% RMSD < 1 Å						% $\mathcal{D} < 0.47$						
	L1	L2	L3	H1	H2	H3	L1	L2	L3	H1	H2	H3	
1	Random	0.518	0.603	0.417	0.221	0.321	0.152	0.669	0.770	0.459	0.597	0.435	0.157
	No CL loss	0.866	0.732	0.714	0.418	0.697	0.305	0.915	0.967	0.836	0.686	0.898	0.464
	No DT filter	0.877	0.748	0.673	0.452	0.680	0.330	0.919	0.994	0.789	0.862	0.882	0.539
	Sequence only	0.790	0.740	0.666	0.413	0.472	0.219	0.809	0.956	0.719	0.750	0.557	0.292
	Dihedral angles only	0.870	0.702	0.591	0.557	0.590	0.298	0.945	0.936	0.752	0.841	0.741	0.491
	Mismatched length	0.878	0.734	0.749	0.593	0.701	0.339	0.941	0.993	0.870	0.834	0.928	0.523
	IGLOO	0.871	0.748	0.761	0.603	0.691	0.327	0.935	0.993	0.856	0.885	0.918	0.669
5	Random	0.558	0.556	0.387	0.229	0.347	0.138	0.679	0.742	0.401	0.561	0.480	0.136
	No CL loss	0.826	0.724	0.636	0.420	0.611	0.279	0.897	0.973	0.765	0.677	0.881	0.413
	No DT filter	0.829	0.748	0.629	0.453	0.646	0.315	0.904	0.996	0.784	0.788	0.876	0.506
	Sequence only	0.798	0.704	0.569	0.401	0.477	0.203	0.844	0.909	0.663	0.633	0.573	0.245
	Dihedral angles only	0.837	0.682	0.611	0.463	0.565	0.280	0.894	0.917	0.759	0.786	0.728	0.454
	Mismatched length	0.828	0.740	0.646	0.473	0.627	0.316	0.897	0.993	0.828	0.643	0.833	0.495
	IGLOO	0.841	0.743	0.666	0.501	0.658	0.315	0.909	0.993	0.827	0.805	0.923	0.553
10	Random	0.550	0.556	0.384	0.235	0.345	0.132	0.666	0.726	0.399	0.556	0.499	0.133
	No CL loss	0.796	0.723	0.601	0.424	0.559	0.265	0.866	0.975	0.724	0.672	0.795	0.376
	No DT filter	0.802	0.744	0.584	0.460	0.600	0.302	0.884	0.994	0.717	0.728	0.840	0.470
	Sequence only	0.781	0.705	0.503	0.391	0.494	0.198	0.852	0.898	0.571	0.655	0.613	0.239
	Dihedral angles only	0.812	0.672	0.595	0.442	0.541	0.263	0.880	0.905	0.715	0.757	0.710	0.400
	Mismatched length	0.804	0.737	0.604	0.469	0.564	0.304	0.867	0.992	0.735	0.671	0.759	0.462
	IGLOO	0.809	0.742	0.623	0.473	0.620	0.300	0.879	0.993	0.764	0.736	0.854	0.473
20	Random	0.545	0.557	0.373	0.249	0.351	0.127	0.648	0.730	0.392	0.559	0.508	0.126
	No CL loss	0.780	0.689	0.516	0.410	0.496	0.242	0.845	0.927	0.603	0.649	0.700	0.335
	No DT filter	0.788	0.704	0.543	0.459	0.562	0.279	0.860	0.950	0.635	0.686	0.747	0.417
	Sequence only	0.761	0.693	0.484	0.400	0.482	0.193	0.828	0.887	0.533	0.614	0.624	0.217
	Dihedral angles only	0.795	0.651	0.524	0.424	0.497	0.245	0.853	0.884	0.617	0.702	0.671	0.356
	Mismatched length	0.789	0.703	0.533	0.465	0.538	0.280	0.843	0.954	0.627	0.689	0.749	0.408
	IGLOO	0.793	0.705	0.558	0.459	0.578	0.278	0.851	0.956	0.674	0.715	0.749	0.402

Dihedral distance contrastive loss. Key to the IGLOO approach is the contrastive learning objective for the model to learn to place loops that share similar backbone dihedral angles in the same region of the latent space. To test this component of the model, we removed the dihedral contrastive loss from training. Consequently, the ablated model is only focused on the reconstruction of masked

Algorithm 1 Dihedral angle distance between a pair of loops of different lengths

Input: loop dihedral angles $\phi_1, \psi_1, \omega_1 \in (-\pi, \pi]^n$, $\phi_2, \psi_2, \omega_2 \in (-\pi, \pi]^m$; loop C_α coordinates $\mathbf{L}_1 \in \mathbb{R}^{n \times 3}$, $\mathbf{L}_2 \in \mathbb{R}^{m \times 3}$; stem C_α coordinates $\mathbf{S}_1, \mathbf{S}_2 \in \mathbb{R}^{N_{\text{stem}} \times 3}$; tolerance k (max. residue length difference)

Output: dihedral angle distance $\mathcal{D} \in [0, 4]$

```
1: if  $|n - m| > k$  then
2:   return 4.0 ▷ returns  $\mathcal{D}_{\text{max}}$ 
3: end if
4:  $\boldsymbol{\mu}_1 \leftarrow \text{mean}(\mathbf{S}_1)$ ;  $\boldsymbol{\mu}_2 \leftarrow \text{mean}(\mathbf{S}_2)$ 
5:  $\tilde{\mathbf{S}}_1 \leftarrow \mathbf{S}_1 - \boldsymbol{\mu}_1$ ;  $\tilde{\mathbf{S}}_2 \leftarrow \mathbf{S}_2 - \boldsymbol{\mu}_2$ 
6:  $(\mathbf{R}, \mathbf{t}, \text{RMSD}_{\text{stem}}) \leftarrow \text{Kabsch}(\tilde{\mathbf{S}}_1, \tilde{\mathbf{S}}_2)$ 
7: if  $\text{RMSD} > 1.0 \text{ \AA}$  then
8:   return 4.0 ▷ returns  $\mathcal{D}_{\text{max}}$ 
9: end if
10:  $\tilde{\mathbf{L}}_1 \leftarrow (\mathbf{L}_1 - \boldsymbol{\mu}_1)\mathbf{R}^\top + \boldsymbol{\mu}_2 + \mathbf{t}$ ;  $\tilde{\mathbf{L}}_2 \leftarrow \mathbf{L}_2$ 
11:  $\mathcal{P} \leftarrow \text{DTW}(\tilde{\mathbf{L}}_1, \tilde{\mathbf{L}}_2)$  ▷ warping path  $\mathcal{P}$  mapping residues of  $\mathbf{L}_1$  to  $\mathbf{L}_2$ 
12:  $\tilde{\phi}_1 \leftarrow \mathcal{P}(\phi_1)$ ;  $\tilde{\psi}_1 \leftarrow \mathcal{P}(\psi_1)$ ;  $\tilde{\omega}_1 \leftarrow \mathcal{P}(\omega_1)$ ;
13:  $\mathcal{D}_\phi \leftarrow \text{mean}(2(1 - \cos(\tilde{\phi}_1 - \phi_2)))$ ;  $\mathcal{D}_\psi \leftarrow \text{mean}(2(1 - \cos(\tilde{\psi}_1 - \psi_2)))$ ;  $\mathcal{D}_\omega \leftarrow$   

    $\text{mean}(2(1 - \cos(\tilde{\omega}_1 - \omega_2)))$ 
14:  $\mathcal{D} \leftarrow \text{mean}(\mathcal{D}_\phi, \mathcal{D}_\psi, \mathcal{D}_\omega)$ 
15: return  $\mathcal{D}$ 
```

amino acids and dihedral angles. We observed in Table S3 that the contrastive learning objective improves performance across loop regions on both precision for $\text{RMSD} < 1 \text{ \AA}$ and $\mathcal{D} < 0.47$, with improvements of 11.8% on the L3 loop and 20.0% on the H3 loop in precision at rank 20.

Distance-threshold filtering of positive ($\mathcal{D} < 0.1$) and negative ($\mathcal{D} > 0.47$) pairs. \mathcal{D} is a continuous measure of the difference in dihedral angles between two loop backbones. In order for the model to not overfit to an arbitrary threshold of 0.47, which was established by Kelow et al. (2022), we established a distance-threshold filter where loops with $0.1 \leq \mathcal{D} \leq 0.47$ are ignored. We train an ablated model where positive ($\mathcal{D} \leq 0.47$) and negative ($\mathcal{D} > 0.47$) pairs and find that performance is generally comparable to when distance-thresholding is applied, with IGLOO offering slight improvements across most loop types.

Multimodal learning in IGLOO. In IGLOO the input to the transformer is $\mathbf{X} = \mathbf{D} + \mathbf{A}$, in this section we remove the dihedral angles, \mathbf{D} , and sequence, \mathbf{A} , from the model separately. We also adjust the loss function correspondingly. The masked reconstruction of dihedral angles and the masked reconstruction of amino acid identities objectives are also removed, respectively. In Table S3, we observe the dihedral angle modality is most important to the retrieval task, notably for the H3 loop retrieval with an improvement of 85.2%. The addition of the sequence modality is also helpful with improvements observed for almost all loop types and on H3 loop retrieval, an improvement of 12.7% is observed.

D IGLOO WITH MISMATCHED LOOP LENGTH

The IGLOO contrastive loss function only assigns positive labels to pairs of loops of the same length. However, Nowak et al. (2016) explore CDR clusters with loops of multiple lengths, and find clusters L1–10,11,12-A; L1–13,14-A; L3–9,10-A; and L3–10,11-A with loops of different lengths. In this section, we show how IGLOO can be trained to align loops of different lengths in the latent space.

To define positive pairs for loops of different lengths, we use the approach from Nowak et al. (2016). Loops are aligned by the C_α coordinates of their stem region, which we define as the N_{stem} amino acids before and after the loop. We then use dynamic time warping (DTW) (Giorgino, 2009) to determine an alignment between the loop C_α coordinates. For the aligned residues, the dihedral distance \mathcal{D} is calculated (Algorithm 1). Finally, positive and negative pairs are defined by thresholds on \mathcal{D} .

We train the IGLOO architecture with $N_{\text{stem}} = 5$ and tolerance $k = 1$, which is consistent with the multi-length clusters found by Nowak et al. (2016). For batches in an epoch, we find on average 5.0% of pairs of loops in the batch to be of different lengths and $\mathcal{D} < 0.1$. In Table S3 we observe that training IGLOO with positive pairs defined between loops of different lengths leads to a slight decay in performance on most loop types.

E ADDITIONAL RESULTS

E.1 PARATOPE RETRIEVAL

We present additional results for the retrieval of similar loops evaluated with precision at rank 1, 5, and 10 (Table S4).

Table S4: Average precision at rank 1, 5, and 10 for retrieval of similar CDR paratopes. Models are shown in rows. The **first**, **second**, and **third** best performance for each column are highlighted.

# Loops retrieved	% RMSD < 1 Å						% $\mathcal{D} < 0.47$						
	L1	L2	L3	H1	H2	H3	L1	L2	L3	H1	H2	H3	
1	ESM C	0.765	0.747	0.561	0.420	0.670	0.242	0.860	0.969	0.533	0.549	0.786	0.254
	ESM-2 (3B)	0.706	0.733	0.525	0.420	0.586	0.238	0.793	0.960	0.505	0.566	0.867	0.228
	AbLang2	0.766	0.747	0.535	0.384	0.567	0.191	0.835	0.919	0.533	0.575	0.825	0.212
	IgBert	0.802	0.733	0.621	0.410	0.428	0.194	0.853	0.971	0.597	0.528	0.653	0.252
	SaProt	0.804	0.747	0.696	0.475	0.525	0.271	0.877	0.969	0.722	0.733	0.674	0.341
	ProstT5	0.791	0.748	0.729	<i>0.531</i>	<u>0.703</u>	0.331	<i>0.920</i>	0.987	0.878	0.748	0.871	0.487
	MIF	<u>0.879</u>	0.747	0.643	<u>0.557</u>	0.564	0.290	0.915	0.991	0.806	<u>0.911</u>	0.837	0.381
	ProteinMPNN	0.863	0.733	0.706	0.468	0.693	<i>0.355</i>	0.906	0.958	0.798	0.915	<i>0.900</i>	<i>0.543</i>
	Foldseek 3Di	0.840	0.748	<u>0.739</u>	0.509	0.713	<u>0.361</u>	0.947	0.994	<u>0.859</u>	0.771	0.874	0.585
	Amino Aseed	0.890	0.734	<i>0.738</i>	0.462	<i>0.703</i>	0.374	0.907	0.994	0.824	0.787	<u>0.910</u>	0.528
IGLOO	<i>0.871</i>	<i>0.748</i>	0.761	0.603	0.691	0.327	<u>0.935</u>	<u>0.993</u>	<i>0.856</i>	<i>0.885</i>	0.918	0.669	
5	0.765	0.710	0.610	0.408	0.627	0.214	0.842	0.900	0.619	0.658	0.748	0.256	
	ESM-2 (3B)	0.730	0.711	0.540	0.447	0.562	0.225	0.837	0.910	0.607	0.697	0.788	0.251
	AbLang2	0.720	0.717	0.588	0.402	0.563	0.188	0.786	0.896	0.595	0.604	0.816	0.238
	IgBert	0.776	0.709	0.570	0.397	0.578	0.182	0.845	0.938	0.566	0.677	0.798	0.259
	SaProt	0.782	0.741	0.607	0.441	0.552	0.246	0.858	0.970	0.654	0.698	0.753	0.316
	ProstT5	0.805	0.745	0.643	<i>0.499</i>	<u>0.671</u>	0.302	0.879	<i>0.985</i>	0.772	0.742	<i>0.841</i>	0.445
	MIF	0.825	0.739	0.652	0.470	0.571	0.263	<u>0.886</u>	0.985	0.787	0.755	0.750	0.361
	ProteinMPNN	<u>0.851</u>	0.742	0.651	0.482	0.648	<i>0.327</i>	0.878	0.974	0.787	<i>0.762</i>	0.836	<i>0.472</i>
	Foldseek 3Di	0.810	0.742	0.666	0.530	0.680	<u>0.326</u>	<u>0.886</u>	0.985	<u>0.815</u>	<u>0.784</u>	<u>0.869</u>	<u>0.475</u>
	Amino Aseed	0.852	<u>0.745</u>	<u>0.657</u>	0.469	0.606	0.336	0.870	0.994	<i>0.813</i>	0.736	0.825	0.469
IGLOO	<i>0.841</i>	<i>0.743</i>	0.666	<u>0.501</u>	<i>0.658</i>	0.315	0.909	<u>0.993</u>	0.827	0.805	0.923	0.553	
10	0.768	0.705	0.537	0.418	0.583	0.202	0.828	0.921	0.572	0.678	0.768	0.230	
	ESM-2 (3B)	0.744	0.713	0.521	0.439	0.561	0.210	0.837	0.895	0.569	0.716	0.734	0.237
	AbLang2	0.719	0.686	0.522	0.408	0.553	0.186	0.799	0.844	0.558	0.611	0.764	0.228
	IgBert	0.727	0.691	0.520	0.416	0.542	0.182	0.806	0.920	0.541	0.708	0.726	0.245
	SaProt	0.749	0.733	0.561	0.439	0.551	0.237	0.816	0.961	0.653	0.722	0.730	0.277
	ProstT5	0.799	0.744	0.597	<u>0.499</u>	<i>0.615</i>	0.291	<i>0.870</i>	0.974	0.713	0.731	0.771	0.404
	MIF	0.796	0.732	0.606	0.463	0.529	0.253	0.864	<u>0.984</u>	0.719	0.714	0.675	0.337
	ProteinMPNN	<u>0.821</u>	<u>0.742</u>	0.601	<i>0.481</i>	0.570	<u>0.310</u>	0.865	0.980	0.719	0.751	0.765	<i>0.419</i>
	Foldseek 3Di	0.800	0.728	0.630	0.508	0.635	<i>0.307</i>	<u>0.873</u>	0.959	<u>0.750</u>	0.751	0.797	0.416
	Amino Aseed	0.830	<u>0.742</u>	<i>0.619</i>	0.453	0.599	0.318	0.869	0.993	<i>0.738</i>	0.717	<u>0.822</u>	0.427
IGLOO	<i>0.809</i>	<i>0.742</i>	0.623	0.473	0.620	0.300	0.879	0.993	0.764	<u>0.736</u>	0.854	0.473	

E.2 LOOPS WITH NO KNOWN CANONICAL CLUSTER

Table S5: Proportion of loops in SabDab with no known Kelow et al. (2022) canonical cluster with a cutoff of $\mathcal{D} = 0.47$ to cluster centroids.

CDR	Heavy	Light
CDR1	0.130	0.112
CDR2	0.098	0.187
CDR3	0.763	0.192
CDR4	0.037	0.062

E.3 VISUALIZATION OF IGLOO LATENT SPACE

In Fig. S1 we visualize the IGLOO token \mathbf{t} for all loops in SabDab across train, test, and validation datasets in 2D with Uniform Manifold Approximation and Projection (UMAP) (McInnes et al., 2018). We observe in the UMAP that the embeddings are localized by their loop type, loop length, and canonical cluster. Among the CDRs, the H3 embeddings span the broadest region of the UMAP manifold, reflecting their markedly higher structural diversity.

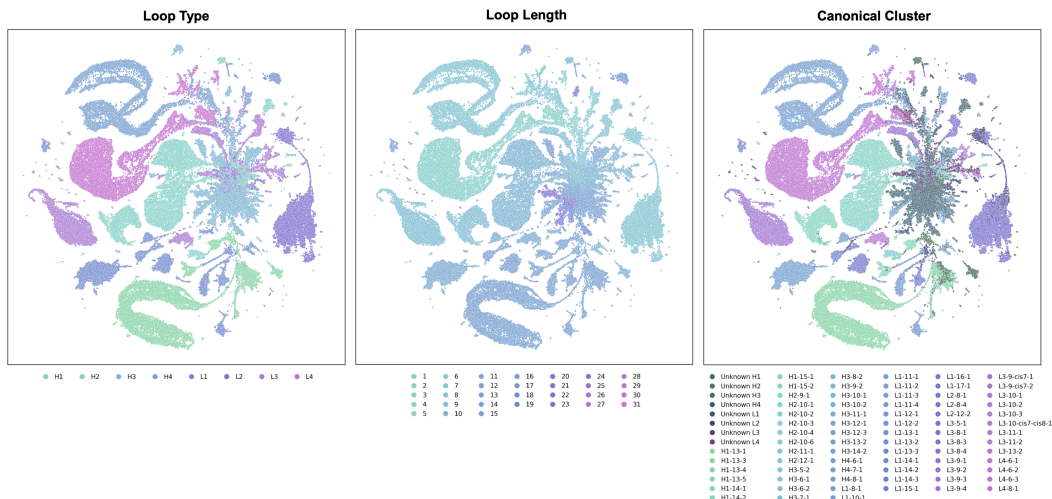


Figure S1: UMAP of the IGLOO latent space for loops in SAbDab. **Left** Loops colored by loop type. **Middle** Loops colored by loop length. **Right** Loops colored by their canonical cluster.

E.4 RECOVERY OF THE CANONICAL CLUSTERS

In Table S6 we report how well IGLOO can recover Kelow et al. (2022) clusters based on the IGLOO quantized token, \hat{t} . We compare the results with (1) IGLOO with the dihedral angles masked out and only sequence input, and (2) IGLOO with the sequence masked out and only dihedral angles input. IGLOO performs best when dihedral angles are provided, though the dihedral angles can also be obtained through protein structure prediction models. Inference with only sequence input is suitable when encoding large libraries of antibody sequences, where structure prediction would be too computationally intensive. We observe that the performance of the sequence-only IGLOO is very close to the IGLOO model for most loop types except for the H3 and L3 loops.

Table S6: Average IGLOO cluster purity (\uparrow) of North et al. (2011) defined clusters of antibody CDRs across SAbDab.

Loop Type	IGLOO	IGLOO sequence only	IGLOO dihedral angles only
H1	0.894	0.880	0.898
H2	0.900	0.875	0.914
H3	0.754	0.537	0.725
H4	0.983	0.996	0.979
L1	0.880	0.841	0.867
L2	0.975	0.991	0.976
L3	0.831	0.771	0.812
L4	0.930	0.928	0.914

E.5 PREDICTING BINDING AFFINITY WITH IGLOO TOKENS

In Table S7, we show results of IGLOOALM compared to IGLOOLM in predicting binding affinity for AbBiBench. IGLOOALM additionally includes multimodal residue tokens from IGLOO which encode the dihedral angle backbone of the loop residues. We observe a drop in performance when these tokens are added. This is consistent with the lower performance of protein language models which use Foldseek 3Di tokens (SaProt and ProstT5 in Table 3). In the binding-affinity benchmark, models must distinguish subtle differences among a small set of heavy-chain variants. State-of-the-art structure-prediction models often miss these nuanced conformational changes (Pak et al., 2023; Buel & Walters, 2022), and the resulting errors propagate to protein language models that rely on residue-level structural tokens.

Table S7: Spearman correlation coefficient (\uparrow) for binding affinity prediction on AbBiBench for IGLOOLM and IGLOOALM.

Target	IGLOOLM	IGLOOALM
1mlc	0.616 (0.009)	0.513 (0.020)
1n8z	0.675 (0.025)	0.556 (0.023)
2fjg	0.713 (0.014)	0.635 (0.015)
3gbn_h1	0.948 (0.004)	0.929 (0.005)
3gbn_h9	0.962 (0.003)	0.959 (0.002)
4fqi_h1	0.921 (0.001)	0.886 (0.001)
4fqi_h3	0.971 (0.001)	0.967 (0.001)
aay149	0.625 (0.010)	0.552 (0.007)
aay149_ML	0.531 (0.007)	0.493 (0.007)
aay151	0.579 (0.011)	0.545 (0.014)

E.6 CONTROLLABLE SAMPLING OF ANTIBODY LOOPS

In Figure S2 we present additional examples of IGLOOALM sampled sequences and their predicted structures. We present examples where the sampled loops have on average at most 60% sequence identity with the original loop.

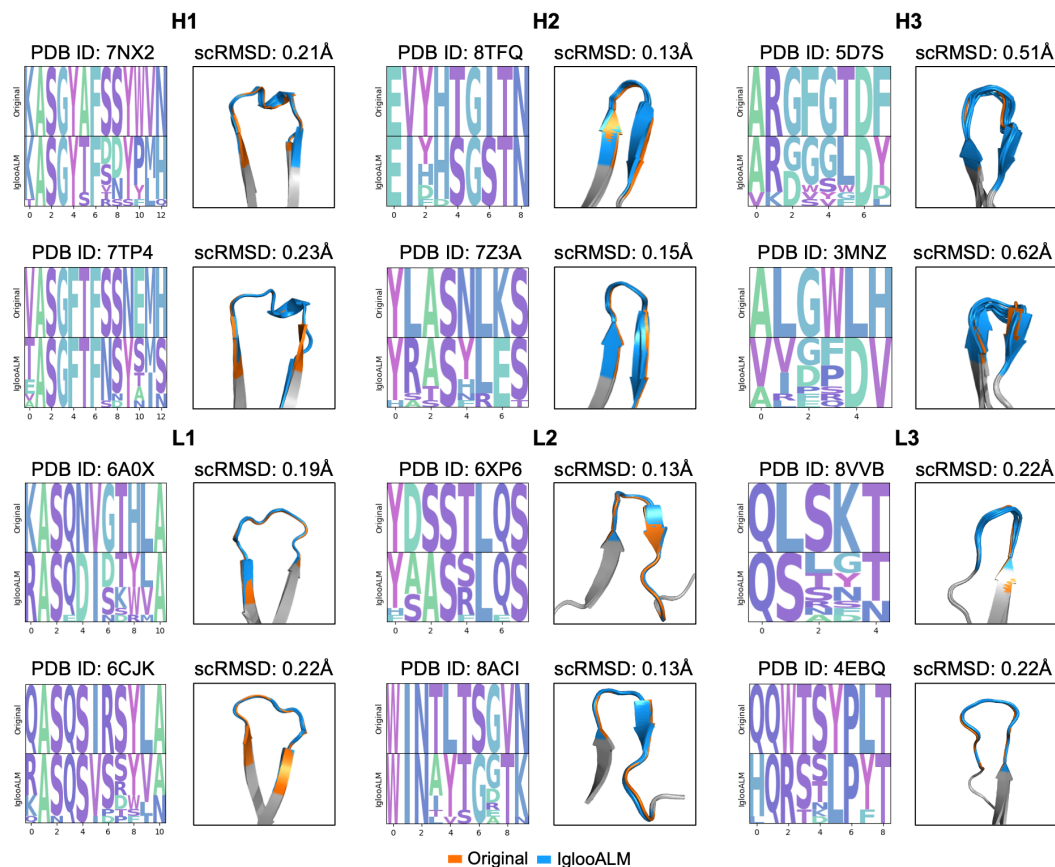


Figure S2: Sequence logo of original and ten IGLOOALM sampled sequences of CDR loop regions at $\lambda = 0.5$ and predicted structures.